



Downloaded from: Dalhousie's Institutional Repository  
DalSpace  
(<http://dalspace.library.dal.ca/>)

Type of print: Publisher Copy  
Originally published: Journal of Geophysical Research  
Permanent handle in DalSpace: <http://hdl.handle.net/10222/24130>

## Three-dimensional model interpretation of $\text{NO}_x$ measurements from the lower stratosphere

Ian Folkins,<sup>1,2</sup> A. J. Weinheimer,<sup>1</sup> Guy Brasseur,<sup>1</sup> Franck Lefèvre,<sup>3</sup> Brian A. Ridley,<sup>1</sup> James G. Walega,<sup>1</sup> James E. Collins,<sup>4</sup> and R. F. Pueschel<sup>5</sup>

**Abstract.** A three-dimensional off-line chemistry transport model, driven by European Centre for Medium-Range Weather Forecasts winds and temperatures, is used to interpret measurements of NO and  $\text{NO}_2$  taken from the DC-8 during the second Airborne Arctic Stratospheric Expedition. The model was run in three configurations: gas phase chemistry alone, inclusion of the  $\text{N}_2\text{O}_5$  aerosol reaction, and inclusion of both  $\text{N}_2\text{O}_5$  and ClONO<sub>2</sub> aerosol reactions. The run including the  $\text{N}_2\text{O}_5$  aerosol reaction alone usually agreed best with measured  $\text{NO}_x/\text{NO}_y$  ratios in midlatitude air masses. The  $\text{NO}_x/\text{NO}_y$  ratios of the run with both aerosol reactions were always too low, while the gas phase ratios were usually too high, especially during March. All three simulations generated extremely low  $\text{NO}_2/\text{NO}_y$  ratios in air parcels that had spent several days or more in the polar night. Measured  $\text{NO}_2/\text{NO}_y$  ratios in these types of air masses were sometimes equally low but could also be considerably higher. Observed NO/ $\text{NO}_2$  ratios differed strongly from known theory.

### Introduction

Two airplanes participated in the second Airborne Arctic Stratospheric Expedition (AASE 2). The ER-2, usually flying at heights of 18-20 km, was able to take measurements in air masses recently exposed to chemical processing by polar stratospheric clouds. The DC-8, flying at altitudes of 10-12 km, sampled air masses at the lowest levels of the stratosphere. This paper uses a three-dimensional model, incorporating the meteorological conditions through which the DC-8 flew, to interpret the DC-8  $\text{NO}_x$  ( $\text{NO} + \text{NO}_2$ ) measurements.

There were 19 DC-8 flights. The first took place on January 8, 1992, and the last on March 20, 1992. A variety of Arctic, midlatitude, and tropical upper tropospheric air masses were sampled. Aerosol levels in the stratospheric air through which the DC-8 flew were considerably above normal, attributable to the eruption of Mount Pinatubo the previous summer [Pueschel *et al.*, 1992]. There is strong evidence that reactions on aerosols lower  $\text{NO}_x/\text{NO}_y$  ratios in the stratosphere [Granier and Brasseur, 1992, Kawa *et al.*, 1993,

Fahey *et al.*, 1993]. Although this may imply that the  $\text{NO}_x$  concentrations measured during the campaign were atypical, it did provide an interesting opportunity to determine the response of this region of the atmosphere to high aerosol loading.

The two sulfate aerosol reactions whose stratospheric importance has been most discussed are the reaction of gaseous  $\text{N}_2\text{O}_5$  with water on the surfaces of sulfuric acid droplets, with the subsequent evaporation of two nitric acid molecules to the gas phase, and the reaction of ClONO<sub>2</sub> with water on the aerosol surface, with the evaporation of an HOCl and nitric acid molecule.



The  $\text{N}_2\text{O}_5$  reaction lowers  $\text{NO}_x/\text{NO}_y$  because nitric acid photolyzes much less readily than  $\text{N}_2\text{O}_5$ . One reason for the current interest in clarifying the status of this reaction is that total ozone concentrations in models become more sensitive to changes in total chlorine levels when this reaction is included [Rodríguez *et al.*, 1991; Granier and Brasseur, 1992]. This is the first investigation of (R1) using  $\text{NO}_x$  measurements taken immediately above the tropopause. As such, it is of particular significance for the effects of aircraft emissions on  $\text{NO}_x$  levels.

The probability that a ClONO<sub>2</sub> molecule colliding with an aerosol will subsequently react with a water molecule depends strongly on the water content of the aerosol. The chemical signature of the ClONO<sub>2</sub> reaction is expected to be too small to detect under most circumstances because the aerosols are too acidic. Its status has therefore been more uncertain than the  $\text{N}_2\text{O}_5$  reaction. However, a recent report has attributed large OClO column abundances observed in the Antarctic fall to this reaction [Solomon *et al.*, 1993]. Another re-

<sup>1</sup>National Center for Atmospheric Research, Boulder, Colorado.

<sup>2</sup>Now at Department of Oceanography, Dalhousie University, Halifax, Nova Scotia, Canada.

<sup>3</sup>Météo-France, Centre National de Recherches Météorologiques, Toulouse, France.

<sup>4</sup>Science and Technology Corporation, Hampton, Virginia.

<sup>5</sup>NASA Ames Research Center, Moffett Field, California.

Copyright 1994 by the American Geophysical Union.

Paper number 94JD01617.  
0148-0227/94/94JD-01617\$05.00

cent study has noted that the reaction probability of the ClONO<sub>2</sub> reaction will usually be largest just above the Arctic winter tropopause [Hofmann and Oltmans, 1992], the region of the stratosphere where aerosols tend to be most dilute. Since aerosol surface areas were considerably above normal during the flight period, the DC-8 measurements provide a good opportunity to look for the effects of this reaction.

## Instrumentation

NO, NO<sub>2</sub>, NO<sub>y</sub> (including peroxy acetyl nitrate), and O<sub>3</sub> were measured using a four-channel chemiluminescence instrument [Walega *et al.*, 1991]. Signals were accumulated and recorded over 2-s intervals; 1-min averages are reported here. Levels of NO<sub>y</sub> and O<sub>3</sub> were well above the detection limits of the instruments, and overall uncertainties including known, quantifiable errors were generally less than 10 and 5 %, respectively. Levels of NO and NO<sub>2</sub> were frequently near detection limits, so error estimates are critical for some of the comparisons to be made later. Errors are variable, but some typical values of the 1-sigma errors in 1-min values are presented here. At 10-12 km and for low levels of NO the precision of the NO instrument is 5 ppt, and the overall uncertainty is better than 10 ppt. For NO<sub>2</sub> the errors depend on ambient NO. For the range 0-30 ppt NO and low NO<sub>2</sub>, the NO<sub>2</sub> precision is 10 ppt, and the overall uncertainty is about 25 ppt. Thus when NO<sub>y</sub> is 1500 ppt and NO and NO<sub>2</sub> are near zero, the precisions in NO/NO<sub>y</sub> and NO<sub>2</sub>/NO<sub>y</sub> are 0.003 and 0.007, and the overall uncertainties are 0.007 and 0.017. For the comparisons that follow, the systematic (sensitivity and artifact) error is most important and is generally about half the overall uncertainty.

The NO<sub>2</sub> measurement relies on broadband photolysis for the conversion of ambient NO<sub>2</sub> to NO prior to detection. Thus there is the potential of interferences from other species. Using the spectrum of the Xe arc lamp [Kley and McFarland, 1980] and current cross sections [deMore *et al.*, 1992], the degree of photolysis of potential interferences can be calculated. Fractions photolyzed during the 5-s residence time in the photolysis cell are 0.7 % for N<sub>2</sub>O<sub>5</sub>, 0.8 % for ClONO<sub>2</sub>, 0.2 % for HO<sub>2</sub>NO<sub>2</sub>, and 16 % for HONO. A filter which attenuates light of less than 320 nm is used to prevent photolysis of HNO<sub>3</sub>. Homogeneous thermal dissociation can also be calculated (using deMore *et al.* [1992]) for both the 5 s in the photolysis cell (at 5 °C) and the 0.2 s in the heated inlet (35 °C). For N<sub>2</sub>O<sub>5</sub> and HO<sub>2</sub>NO<sub>2</sub>, total fractions dissociated are each 2-3 %. Thus interference due to homogeneous processes is small. However, heterogeneous dissociation is also possible and has yet to be tested in the laboratory, so the NO<sub>2</sub> measurements must be regarded as upper limits.

## Model Description

The model was a modified version of a chemistry transport model previously used to assess the extent of ozone depletion during the 1991-1992 winter [Lefèvre

*et al.*, 1994]. The main modification was to change the vertical domain from 10-50 km to 6-16 km, in 2-km pressure height intervals. The northern hemisphere was covered with 2° resolution in the meridional direction and 2.5° in the zonal. Horizontal winds and temperatures were linearly interpolated in time from stored 12 hourly European Centre for Medium-Range Weather Forecasts (ECMWF) data, which had 2.5° resolution in both horizontal directions and nonuniform vertical resolution, so that some interpolation to the model grid was required. The vertical winds were solved, at each time step during the model run, from the continuity equation using the interpolated horizontal winds.

The 40 model species were divided into two categories: 28 transported species and 12 short-lived species determined from photochemical equilibrium expressions. With the exception of atomic nitrogen the 12 short-lived species were grouped together into five transported families: O<sub>x</sub> (O<sup>1</sup>D, O, and O<sub>3</sub>), HO<sub>x</sub> (OH and HO<sub>2</sub>), NO<sub>x</sub> (NO and NO<sub>2</sub>), ClO<sub>x</sub> (Cl and ClO), and BrO<sub>x</sub> (Br and BrO). The sum of the transported reactive nitrogen compounds, which in addition to NO<sub>x</sub> included HNO<sub>3</sub>, N<sub>2</sub>O<sub>5</sub>, NO<sub>3</sub>, HO<sub>2</sub>NO<sub>2</sub>, ClONO<sub>2</sub>, ClNO<sub>2</sub>, and BrONO<sub>2</sub>, was normalized at every time step (every 7.5 min) to the transported value of NO<sub>y</sub>, as were the transported reactive chlorine compounds, ClONO<sub>2</sub>, ClNO<sub>2</sub>, ClO<sub>x</sub>, OClO, HCl, HOCl, Cl<sub>2</sub>, BrCl, and Cl<sub>2</sub>O<sub>2</sub>, to Cl<sub>y</sub>. Total bromine, defined as the sum of BrO<sub>x</sub>, BrCl, BrONO<sub>2</sub>, HOBr, and HBr, was fixed at 0.54 % of Cl<sub>y</sub> [World Meteorological Organization, (WMO) 1992]. The remaining transported species were N<sub>2</sub>O, CH<sub>4</sub>, H<sub>2</sub>O, CO, CFC-11, CFC-12, H<sub>2</sub>O<sub>2</sub>, and aerosol surface area, which was transported as a passive tracer.

Species were advected by the winds using a semi-Lagrangian scheme. Reaction rates were based on 1992 Jet Propulsion Laboratory recommendations [DeMore *et al.*, 1992]. Methane chemistry was included to the extent that it is a sink of OH, O<sup>1</sup>D, and Cl, but none of the intermediates in its oxidation to CO were represented. The reaction probability of the N<sub>2</sub>O<sub>5</sub> aerosol reaction was taken to be 0.1 [DeMore *et al.*, 1992]. The dependence of the ClONO<sub>2</sub> aerosol reaction probability on aerosol water content was the same as that from Figure 1 of Granier and Brasseur [1992]. Photolysis rates for the model species were obtained from a lookup table specifying the rates as a function of pressure, solar zenith angle, overhead ozone column, and surface albedo. The ozone column at a particular grid point was calculated by subtracting from the Total Ozone Mapping Spectrometer column values [Gaines *et al.*, 1992], the amount of ozone between this grid point, and the bottom model level. A correction of 18 Dobson units was further subtracted from this result as an estimate of the amount of ozone below 6 km. The albedo was everywhere set equal to 0.3.

## Initialization

To analyze airplane measurements taken within weeks of the start of a model run, it is necessary that the initial distributions of the long-lived chemical species be real-

istic. We use a modification of the initialization procedure discussed by *Douglass et al.* [1990]. This technique exploits the high degree of correlation of most long-lived species mixing ratios in the stratosphere with potential temperature (PT) and potential vorticity (PV) [*Schoeberl et al.*, 1989]. PT and PV were calculated at every grid point of the two starting dates (January 1 and March 1) using the initial winds and temperatures. Values of N<sub>2</sub>O, O<sub>3</sub>, H<sub>2</sub>O, NO<sub>y</sub>, aerosol area, and CO were then assigned to each grid point using a mapping between the mixing ratios of each species with PV and PT. These mappings were generated from the ER-2 and DC-8 measurements of these species available on the AASE 2 CD [*Gaines et al.*, 1992]. The average number of flights used to generate each mapping was around 12 and each flight was usually within 3 weeks of the start date of the run. Correlations of methane, CFC-11, and CFC-12 with N<sub>2</sub>O [*Prather and Remsberg*, 1993] were used to generate initial distributions of these species. Total inorganic chlorine Cl<sub>y</sub> and HCl were initialized using relationships with N<sub>2</sub>O obtained during AASE 2 [*Webster et al.*, 1993]. The balance of Cl<sub>y</sub> was assumed to be mostly ClONO<sub>2</sub>. The initial partitioning of NO<sub>y</sub> minus ClONO<sub>2</sub> was taken to be 70% HNO<sub>3</sub>, 20% NO<sub>x</sub>, and 5% N<sub>2</sub>O<sub>5</sub>. The mixing ratios of the remaining species were set to small values.

Two sets of model simulations were done. One set started on January 1 and was run until January 23. The other started on March 1 and was run until the last DC-8 flight on March 20. The February flights were not studied. Because the solar illumination of this month is intermediate between January and March, it was not thought that the NO<sub>x</sub> measurements from these flights would provide insights in addition to those gained from analyzing the January and March flights alone. Three runs were done for each set: a run with gas phase reactions alone (the gas case), a run which also included the N<sub>2</sub>O<sub>5</sub> aerosol reaction (the N<sub>2</sub>O<sub>5</sub> case), and a run with both N<sub>2</sub>O<sub>5</sub> and ClONO<sub>2</sub> aerosol reactions (the ClONO<sub>2</sub> case). For the March runs but not those in January the initial chemical state was subjected to 20 days of chemistry and no transport before the start of the simulation.

The variations of the main NO<sub>y</sub> and Cl<sub>y</sub> species during the 20-day March initialization at the 12 km 37°N and 12.5°E grid point are shown in Figure 1. The mixing ratios of water, NO<sub>y</sub>, Cl<sub>y</sub>, and ozone at this grid point were 6 ppm and 2.2, 0.56, and 484 ppb. The aerosol surface area density was 12 μm<sup>2</sup>/cm<sup>3</sup> and the temperature 215 K. Although Cl<sub>y</sub> was initially partitioned about equally between HCl and ClONO<sub>2</sub> (as given by the ER-2 measurements [*Webster et al.*, 1993]), the model runs drive HCl/Cl<sub>y</sub> to about 0.9. This inconsistency between the model Cl<sub>y</sub> partitioning and the AASE 2 HCl measurements appears to be a generic feature of models. HO<sub>2</sub>NO<sub>2</sub> is not shown in Figure 1 but occupies about 2% of NO<sub>y</sub> in all runs.

The gas phase HNO<sub>3</sub>/NO<sub>y</sub> ratio in Figure 1 decreases throughout the 20-day initialization period, despite the fact that the fraction of NO<sub>y</sub> in the form of ClONO<sub>2</sub> is also steadily decreasing. The HNO<sub>3</sub> decrease is very slow because 24-hour-averaged HNO<sub>3</sub> photolysis

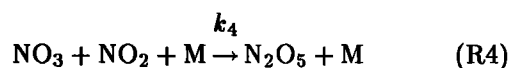
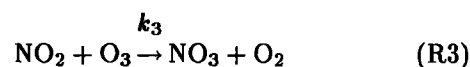
timescales in midlatitudes are about 50 days. Nevertheless, NO<sub>x</sub>/NO<sub>y</sub> ratios appear to be within a few percent of steady state at the end of the 20 days. In the aerosol case, HNO<sub>3</sub>/NO<sub>y</sub> rapidly increases as first N<sub>2</sub>O<sub>5</sub>, and then NO<sub>x</sub>, is converted to nitric acid. The NO<sub>x</sub>/NO<sub>y</sub> ratio undergoes little change between day 5 and day 20 of the initialization run.

The absence of a January chemical initialization is unlikely to have affected modeled NO<sub>x</sub>/NO<sub>y</sub> ratios for the two aerosol runs. Provided one starts with an excess of NO<sub>x</sub> (as was done), the conversion of NO<sub>2</sub> to HNO<sub>3</sub> via the aerosol pathway is sufficiently rapid to drive NO<sub>x</sub>/NO<sub>y</sub> to steady state within a few days. For the gas phase run, the absence of an initialization may have led to an underestimate of NO<sub>x</sub>/NO<sub>y</sub> in those regions where the initial NO<sub>x</sub> was below its photochemical equilibrium value. But since the first January flight analyzed here occurs 14 days after the start of the run (as opposed to 10 days in March), this underestimate is likely to be small.

The ClONO<sub>2</sub> lifetime associated with (R2) was 110 hours at the grid point discussed above. This was considerably longer than the photolysis lifetime, so that the effect of (R2) on Cl<sub>y</sub> and NO<sub>y</sub> partitioning was small. The importance of this reaction increases toward the pole. ClONO<sub>2</sub> within the polar night was almost entirely converted to HOCl during the initialization.

## Saturation

The reactions that generate N<sub>2</sub>O<sub>5</sub> have a direct bearing on NO<sub>x</sub>/NO<sub>y</sub> ratios in both gas phase and aerosol cases. They are



where M refers to the involvement of a third molecule. The second reaction effectively operates only at night because NO<sub>3</sub> photolyzes rapidly. The lifetime of an NO<sub>2</sub> molecule against conversion to NO<sub>3</sub> via (R3), given by  $(k_3[\text{O}_3])^{-1}$  where [O<sub>3</sub>] is the ozone number density, was 80 hours at this grid point. At night the only NO<sub>3</sub> sink in the model is (R4). It can be shown that the NO<sub>3</sub> lifetime associated with this reaction is much shorter than 80 hours unless the NO<sub>2</sub> concentration is extremely small. For the most part, it can be assumed that the production of NO<sub>3</sub> from NO<sub>2</sub> is immediately followed by conversion to N<sub>2</sub>O<sub>5</sub>, so that (R3) represents the loss of two NO<sub>2</sub> molecules, giving rise to an effective NO<sub>2</sub> lifetime of 40 rather than 80 hours.

When the lifetime of an NO<sub>2</sub> molecule associated with conversion to N<sub>2</sub>O<sub>5</sub> via (R3) and (R4) is much longer than the lifetime of N<sub>2</sub>O<sub>5</sub> to subsequently heterogeneously convert to HNO<sub>3</sub>, it is clearly the gas phase reactions that will limit the rate at which HNO<sub>3</sub> can be

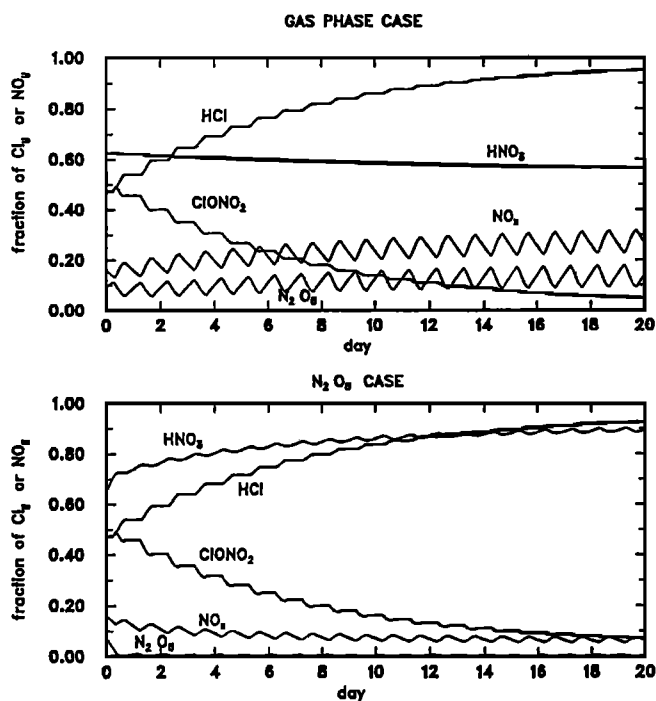


**Figure 1.** The variation of the major members of the NO<sub>y</sub> and Cl<sub>y</sub> families during the 20-day initialization period at the start of the March simulations (perpetual March 1 conditions, no dynamics) at the 37°N and 12.5°E grid point on the 12-km pressure level. ClONO<sub>2</sub> is expressed as a fraction of Cl<sub>y</sub> but is included in NO<sub>y</sub> also. N<sub>2</sub>O<sub>5</sub> is hard to see in the aerosol case because it is so small. Most of the balance of NO<sub>y</sub>, not included in the sum of HNO<sub>3</sub>, NO<sub>x</sub>, 2\*N<sub>2</sub>O<sub>5</sub>, and ClONO<sub>2</sub>, is in the form of HO<sub>2</sub>NO<sub>2</sub>.

produced via the aerosol pathway. Under these circumstances the NO<sub>x</sub>/NO<sub>y</sub> ratio should be insensitive to the N<sub>2</sub>O<sub>5</sub> aerosol reaction probability and surface area (ignoring possible effects on this ratio from the ClONO<sub>2</sub> reaction). This phenomenon is referred to as saturation [Fahey *et al.*, 1993]. The disparity in lifetimes at the grid point discussed above was an order of magnitude (40 versus 4 hours). Since the ozone number density, aerosol surface area, and temperature at this grid point were not atypical, it is likely that the lower stratosphere was saturated throughout the flight period.

## The January Flights

After two short test flights on January 8 and 11 the DC-8 flew from Moffett Field, California, to Anchorage, Alaska, on January 14 and from Anchorage to Stavanger, Norway, two days later. These flight paths are in Plate 1, together with NO<sub>x</sub>/NO<sub>y</sub> on the 12-km model level for January 15. Both gas phase and N<sub>2</sub>O<sub>5</sub> runs show an extensive region of low NO<sub>x</sub>/NO<sub>y</sub> centered on the north pole. The location in the model runs of the boundary between low NO<sub>x</sub> polar air and higher NO<sub>x</sub> midlatitude air is correlated with geopotential height. This can be seen from the plot of ECMWF geopoten-

tial height at 12 km shown in Figure 2. Since NO<sub>x</sub> is conserved with a timescale of several days and the geopotential contours are approximately parallel to the flow streamlines outside the tropics, the tendency of the flow is to bring NO<sub>x</sub> into alignment with the geopotential. The anticyclonic flow of the high-pressure system over England and the cyclonic flow of the low pressure system west of England over the Atlantic are reflected in the model as "double-swirl" patterns in NO<sub>x</sub>. The stretching and folding of material contours occurring within these systems enables mixing between polar and midlatitude air.

Observed and modeled aerosol surface area, ozone, NO<sub>y</sub>, and NO<sub>x</sub>/NO<sub>y</sub> for the January 14 flight are compared in Figure 3. Model values along the DC-8 flight track were obtained by reading in the flight coordinates as the model was run. At each model time step, a value at the flight position was obtained by a linear interpolation to the DC-8 position from the model values at the eight surrounding grid points. The comparison is shown starting at 16 hours, shortly after the plane entered the stratosphere. With the exception of the highly variable tropospheric segments during the dip to 6 km between 18.5 and 19 hours, and after 21.5 hours, aerosol surface area is reasonably well reproduced during this flight. It is not anticipated that the model will reproduce observed NO<sub>x</sub>/NO<sub>y</sub> in the troposphere because of the absence from the model of tropospheric processes. Model ozone and NO<sub>y</sub> are effectively conservative tracers for the duration of the runs, so that the deviations from the measured values seen in Figure 3 reflect either errors in the initialization procedure, the wind fields, or the advection routine. With the exception of the spike just after 19 hours the model tracks these two species reasonably well.

Observed NO<sub>x</sub>/NO<sub>y</sub> ratios during the January 14 flight agreed quite well with the gas phase results during the first half of the flight but were intermediate between the gas phase and N<sub>2</sub>O<sub>5</sub> runs during the second half. Solar zenith angles between 16 and 22 hours were between 85 and 89 degrees. Figure 4 shows both NO/NO<sub>y</sub> and NO<sub>2</sub>/NO<sub>y</sub> along the flight track. With the exception of the tropospheric segments the N<sub>2</sub>O<sub>5</sub> run reproduces the observed variation of NO/NO<sub>y</sub> very well. The discrepancy in NO<sub>x</sub>/NO<sub>y</sub> for this model run is entirely due to an underestimate of NO<sub>2</sub>/NO<sub>y</sub>. All three model runs overpredict the observed NO/NO<sub>2</sub> ratio.

The January 16 flight from Anchorage to Stavanger occurred almost entirely within the polar night. The data for this flight are shown in Figure 5. It gives NO<sub>2</sub>/NO<sub>y</sub> rather than NO<sub>x</sub>/NO<sub>y</sub> since the absence of sunlight meant that measured NO levels were zero to within the uncertainty of the instrument. Low ozone and NO<sub>y</sub> mixing ratios between 7 and 7.5 hours indicate a dip to the troposphere. Observed NO<sub>2</sub>/NO<sub>y</sub> was consistently higher than all three model runs in both the stratosphere and the troposphere.

Although not reproduced by the model, some of the observed NO<sub>2</sub>/NO<sub>y</sub> features appear related to variations in recent exposure to sunlight. Eight-day back



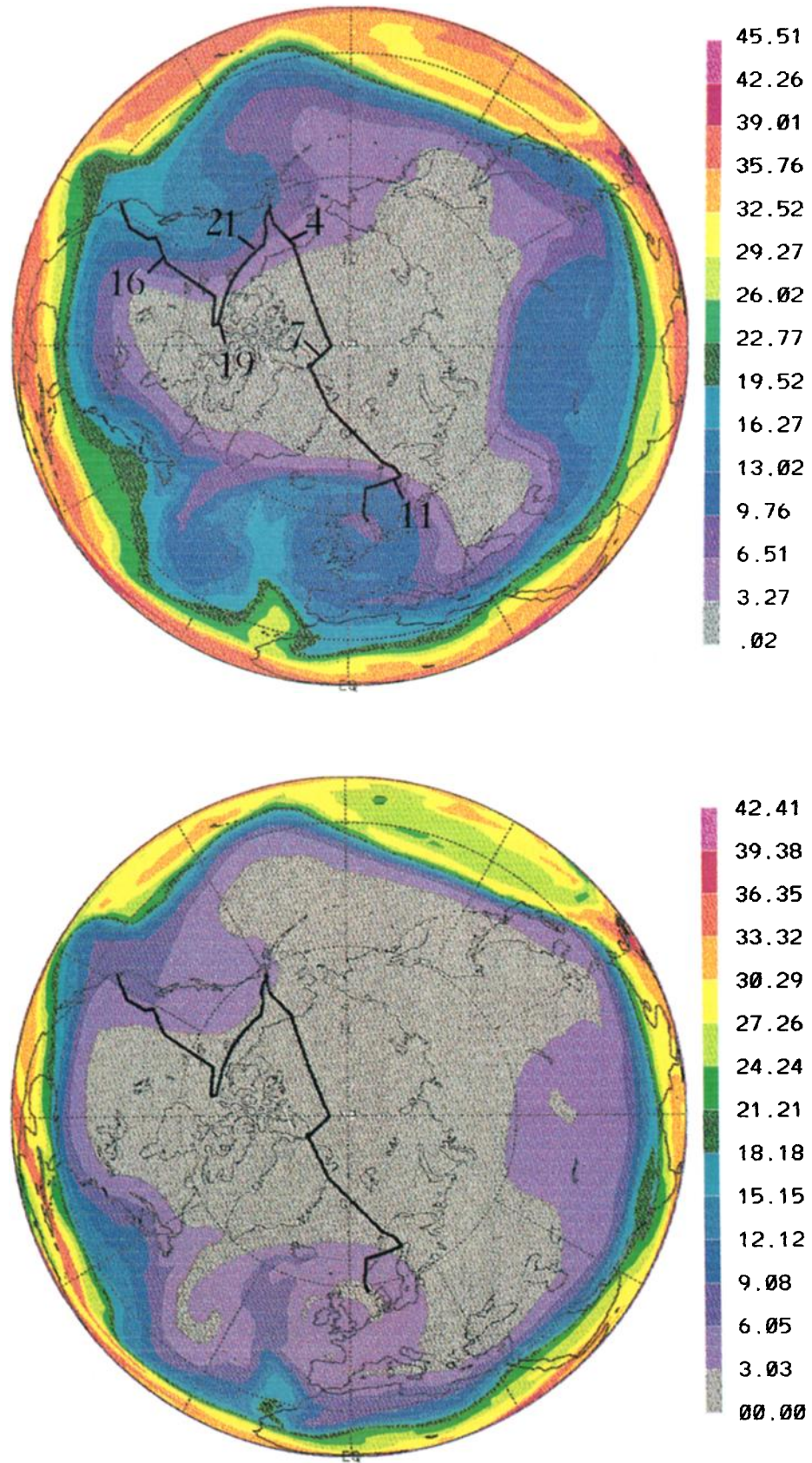


**Plate 1.** Model NO<sub>x</sub>/NO<sub>y</sub> on the 12 km surface at 0000 UT on January 15 for the (a) gas phase run and (b) N<sub>2</sub>O<sub>5</sub> run. Note the differing color scale. The paths of the January 14 flight from Moffett Field to Anchorage and the January 16 flight from Anchorage to Stavanger are shown. The numbers along the flight track in the gas phase case correspond to the time in hours that the plane was at that position.

GPHT at 182.0mb DAY= 15 HOUR= 0

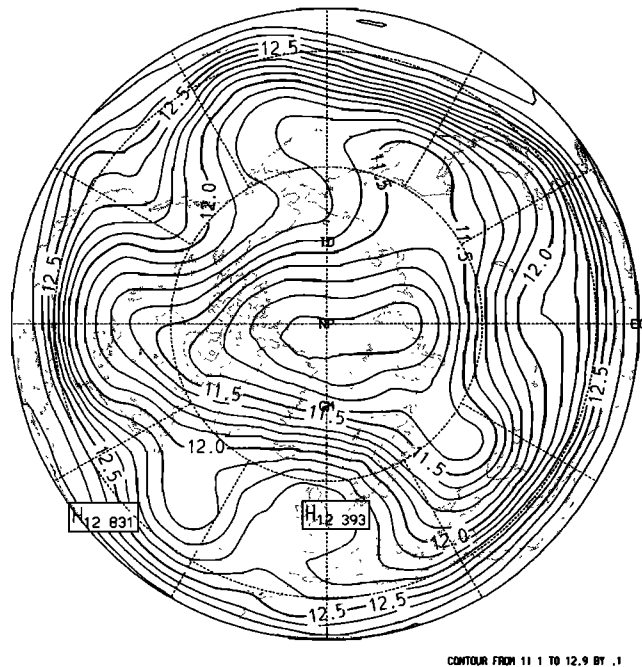


**Figure 2.** European Centre for Medium Range Weather Forecasts geopotential height at 0000 UT January 15 on the 12-km surface. The contour interval is 100 m.

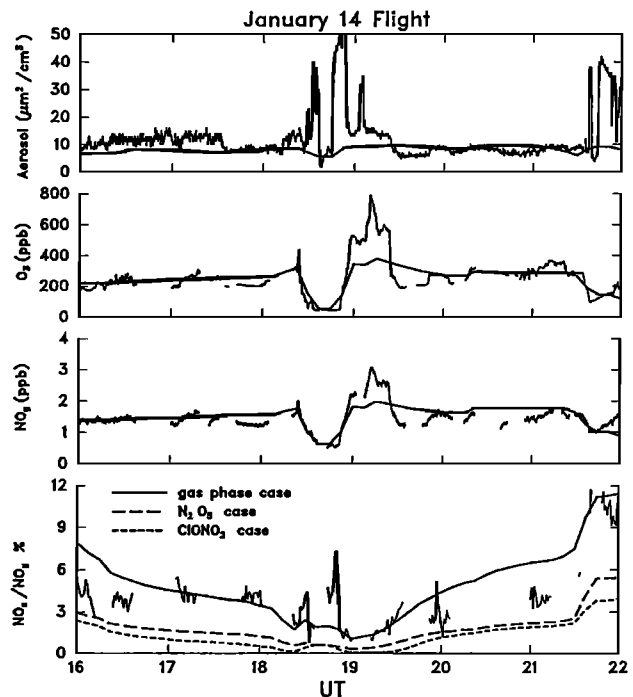
trajectories for this flight are shown in Figure 6. These were computed with the NASA Goddard Space Flight Center back trajectory model using National Meteorological Center (NMC) winds. The circle centered on the north pole denotes the position of the terminator. Figure 5 shows that the highest levels of stratospheric NO<sub>2</sub>/NO<sub>y</sub> occurred just before 6 hours. The back trajectory at this time leaves the polar night after 2 days, ending up at the end of the eight days near the Great Lakes region of North America. It attains the most southerly point of any of the trajectories. In contrast, air parcels intersecting the flight at 5 hours have spent the previous 5 days in darkness, never go far beyond the terminator when they do leave the polar night, and have much lower NO<sub>2</sub>/NO<sub>y</sub>. The back trajectory just before 8 hours has spent the entire 8 days in the polar night and also has very low NO<sub>2</sub>/NO<sub>y</sub>. In going from 8 to 9 hours, the number of days spent in darkness decreases from 9 to 2 but does not give rise to a significant increase in NO<sub>2</sub>/NO<sub>y</sub>.

The low NO<sub>2</sub>/NO<sub>y</sub> ratios in the simulations can be accounted for by the rate at which the model converts NO<sub>2</sub> to N<sub>2</sub>O<sub>5</sub> in the dark [e.g., Ridley *et al.*, 1987; Solomon *et al.*, 1986]. Taking the trajectory just before 8 hours as an example, use of an ozone mixing ratio of 380 ppb and a temperature of 209 K (from the NMC data) implies a lifetime for conversion of NO<sub>2</sub> to NO<sub>3</sub> via (R3) of 94 hours. Assuming sufficient NO<sub>2</sub> for rapid reaction of NO<sub>3</sub> with NO<sub>2</sub> to make N<sub>2</sub>O<sub>5</sub> via (R4) halves this to 47 hours, or approximately 2 days. Since the air parcel following this trajectory had spent 9 days

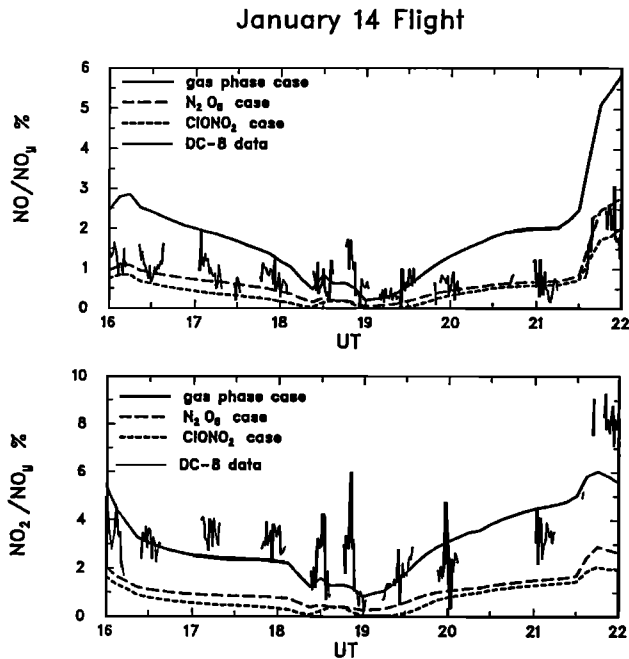
in darkness, its NO<sub>2</sub>/NO<sub>y</sub> should have gone down by a factor of about 100 since entering the polar night. Thermal dissociation of N<sub>2</sub>O<sub>5</sub> and HO<sub>2</sub>NO<sub>2</sub> are far too slow under these conditions to be significant sources of NO<sub>2</sub>. The fact that all three model simulations consistently underestimated observed NO<sub>x</sub>/NO<sub>y</sub> appears to suggest either that the conversion of NO<sub>2</sub> to NO<sub>3</sub> in the model is too fast or that there is a source of NO<sub>2</sub> in the polar night not included in the model.

Figure 7 shows data from the January 23 flight. NO levels were always low because the flight occurred at night. Aerosol surface area was at times considerably higher than measured during previous flights and always higher than the model. This has little effect on model-calculated NO<sub>2</sub>/NO<sub>y</sub> ratios because of the extent to which saturation was in effect. Observed and modeled NO<sub>2</sub>/NO<sub>y</sub> ratios are extremely low from 22.5 hours, when the DC-8 entered the stratosphere, until 26.5 hours. Between 24 and 25 hours the NO<sub>2</sub>/NO<sub>y</sub> ratio was zero to within the uncertainty of the instrument. The range of variability for the low NO<sub>x</sub> portions of this flight, from 0 to 3%, is similar to the 1 to 5% variability for the stratospheric portions of the January 16 flight.

The flight path and 8-day back trajectories for this flight are shown in Figure 8. The back trajectories during the period of low NO<sub>2</sub> have a high degree of curvature and have spent much of the past 8 days traversing



**Figure 3.** Observed and modeled aerosol surface area, ozone, NO<sub>y</sub>, and NO<sub>x</sub>/NO<sub>y</sub> during the January 14 flight. Only gas phase surface area, ozone, and NO<sub>y</sub> are given. These tracers are virtually identical in the other model runs. Observed NO<sub>x</sub>/NO<sub>y</sub> is obtained by adding 1-min averaged NO<sub>2</sub> to 1-min averaged NO and dividing the sum by the NO<sub>y</sub> averaged over the same time interval.



**Figure 4.** Modeled and measured  $\text{NO}/\text{NO}_y$  and  $\text{NO}_2/\text{NO}_y$  during the January 14 flight.

the polar night. Observed  $\text{NO}_2/\text{NO}_y$  increases steadily as the aircraft headed south after 26 hours. This behavior is well reproduced by the aerosol runs, although they underestimate the measurements. The start of the trend toward increased  $\text{NO}_2/\text{NO}_y$  coincides with a change in the character of the back trajectories. They begin to cover much greater distances and intersect the flight from a southerly as opposed to northerly direction.

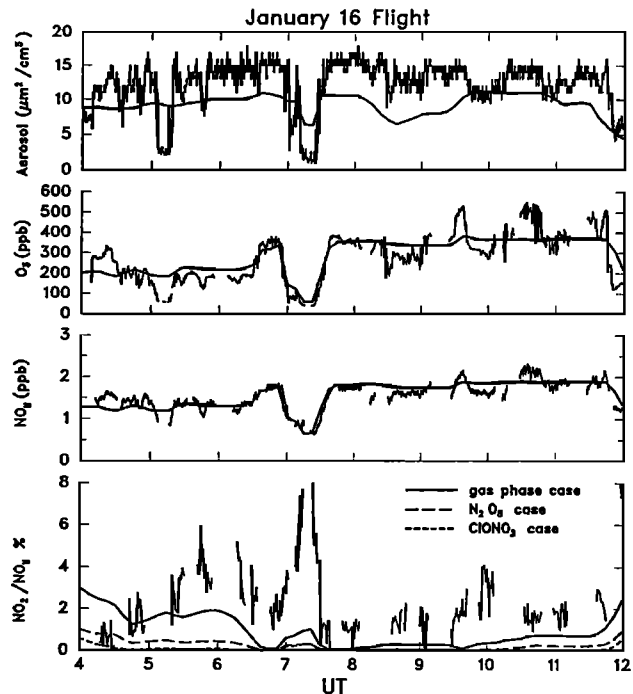
## The March Flights

Plate 2a shows March 11 gas phase  $\text{NO}_x/\text{NO}_y$  on the 12-km surface. The gray low  $\text{NO}_x/\text{NO}_y$  region has shrunk to a fraction of its January size. Its extent is approximately delineated by the size of the polar night. Meridional  $\text{HNO}_3/\text{NO}_y$  gradients tend to be weak in the gas phase model because the main  $\text{HNO}_3$  sink, photolysis, and the main source, the reaction of  $\text{NO}_2$  with  $\text{OH}$ , both tend to be proportional to the amount of sunlight. Meridional gradients in  $\text{NO}_x/\text{NO}_y$  arise largely from interchange between  $\text{NO}_x$  and  $\text{N}_2\text{O}_5$ . Even though the polar night is now much smaller than in January, gas phase conversion of  $\text{NO}_x$  to  $\text{N}_2\text{O}_5$  occurs sufficiently rapidly to make  $\text{NO}_x/\text{NO}_y$  small in the vicinity of the north pole. Air parcels leaving the polar night and encountering sunlight have their  $\text{NO}_x$  quickly restored because  $\text{N}_2\text{O}_5$  photolyzes quite readily. For example, the noon, midlatitude photolysis lifetime is about 11 hours. This gives rise to the rapid increases in  $\text{NO}_x/\text{NO}_y$  seen in Plate 2a along the southward edge of the polar night.

Plate 2b shows March 11  $\text{NO}_x/\text{NO}_y$  on the 12-km surface with the  $\text{N}_2\text{O}_5$  aerosol reaction included. The

gray low  $\text{NO}_x/\text{NO}_y$  region continues to occupy most of the midlatitude regions, much as it did in January. This is because  $\text{HNO}_3$  photolysis is still much slower than  $\text{NO}_x$  to  $\text{HNO}_3$  conversion via the aerosol pathway. The  $\text{N}_2\text{O}_5$  aerosol reaction makes the  $\text{N}_2\text{O}_5/\text{NO}_y$  ratio small, so that meridional gradients in  $\text{NO}_x/\text{NO}_y$  reflect gradients in  $\text{HNO}_3/\text{NO}_y$ , and vice versa. A strong gradient in  $\text{NO}_x/\text{NO}_y$  at the edge of the polar night is not anticipated because  $\text{N}_2\text{O}_5$  concentrations within the polar night are low, due to the aerosol reaction. The increase in contrast between the two cases indicates that the  $\text{NO}_x$  measurements during March provide a better opportunity than those in January for discriminating between the gas phase and the  $\text{N}_2\text{O}_5$  model runs. The green and yellow regions in Plate 2b denote tropospheric air and blue the approximate location of the tropopause. The  $\text{N}_2\text{O}_5$  aerosol reaction is much less effective in suppressing modeled  $\text{NO}_x/\text{NO}_y$  ratios in the troposphere than the stratosphere. This is primarily because ozone concentrations are much lower in the troposphere, so that the conversion of  $\text{NO}_2$  to  $\text{NO}_3$  at night via (R3) occurs much more slowly.

The first March flight occurred on March 10 when the DC-8 flew from Moffett Field to Anchorage. This flight path and the path from Anchorage to Stavanger two days later are shown in Plate 2a. Data from the flight are shown in Figure 9. With the exception of the tropospheric segments shortly after 12 hours and between 14.5 and 15 hours,  $\text{NO}_x/\text{NO}_y$  is best simulated by the  $\text{N}_2\text{O}_5$  run. This run also reproduces the measured  $\text{NO}_x/\text{NO}_y$  gradient as the plane heads south from its point of closest approach to the pole at 15 hours.



**Figure 5.** Modeled and measured tracers and  $\text{NO}_2/\text{NO}_y$  during the January 16 flight. Measured ozone is reported in 1-s intervals.



## Back Trajectories for Jan. 16 Flight

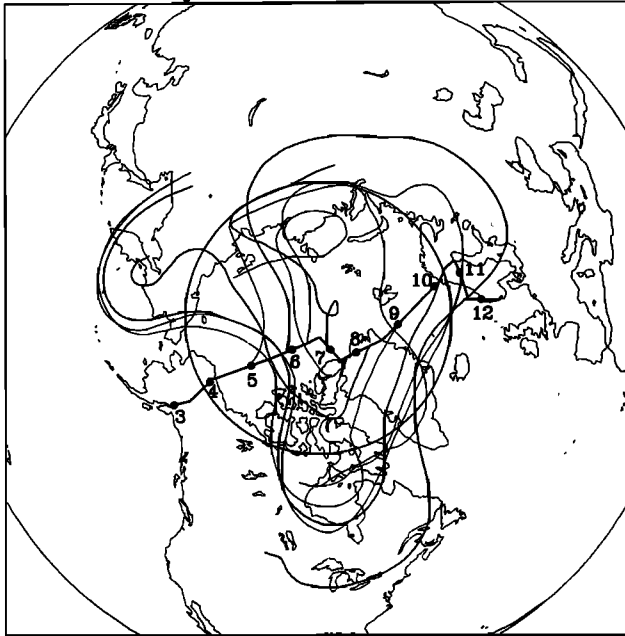


**Figure 6.** Eight-day back trajectories for the January 16 flight. Numbers along the flight path indicate the flight time. Some trajectories are darker than others to help delineate them.

Data from the March 12 flight are shown in Figure 10. With the exception of the tropospheric segment between 4 and 5 hours, NO<sub>x</sub>/NO<sub>y</sub> from the gas phase simulation was again much larger than observed. Ratios from the simulation, including the N<sub>2</sub>O<sub>5</sub> aerosol reaction, were much closer to the measured values but consistently lower. The run with both aerosol reactions generated extremely low NO<sub>x</sub>/NO<sub>y</sub> during all stratospheric portions of the flight.

The last flight of the mission occurred on March 20 when the plane flew from Maine to Moffett Field. Figure 11 shows that NO<sub>x</sub>/NO<sub>y</sub> from the N<sub>2</sub>O<sub>5</sub> model run was again close to but somewhat below the observed ratio. Figure 12, showing both NO/NO<sub>y</sub> and NO<sub>2</sub>/NO<sub>y</sub>, indicates that the underestimate of NO<sub>x</sub>/NO<sub>y</sub> in the N<sub>2</sub>O<sub>5</sub> simulation arises from a lack of NO<sub>2</sub> rather than NO. This is consistent with the January 14 comparison and indicates that the model NO<sub>x</sub> partitioning is different from the observed.

Figure 13 shows gas phase and observed NO/NO<sub>2</sub> from the March 20 flight. In the model this ratio is given to a good approximation by

$$\frac{\text{NO}}{\text{NO}_2} = \frac{J_{\text{NO}_2}}{k_5[\text{O}_3] + k_6[\text{HO}_2] + k_7[\text{ClO}]} \quad (1)$$

where  $k_5$ ,  $k_6$ , and  $k_7$  are the rate constants of the reactions of NO with O<sub>3</sub>, HO<sub>2</sub>, and ClO. The  $k_5$  reaction is dominant by far, so that even though the aerosol reactions tend to increase both HO<sub>2</sub> and ClO, their NO/NO<sub>2</sub> ratios are similar. At 14 hours for example,

NO/NO<sub>2</sub> in the simulation with both aerosol reactions was 13% below the gas phase ratio. This decrease was primarily associated with an increase of ClO from 0.713 to 13.8 ppt. The levels of ClO needed to bring about agreement with the observed ratio would appear to be unrealistic. Figure 11 indicates that the model typically underestimated observed ozone by 15% between 12 and 16 hours. More realistic ozone levels in the model would have also reduced modeled NO/NO<sub>2</sub> somewhat but much less than that needed to overcome the factor of 2 discrepancy seen in Figure 13. The discrepancy is also larger than the known uncertainty in measured NO/NO<sub>2</sub> of 500% or less during the 14 to 16-hour period when NO<sub>2</sub> is highest (about 100 ppt).

The observed March 20 NO/NO<sub>2</sub> ratio has also been compared with the ratio predicted by a simple zero-dimensional model. This model calculates NO/NO<sub>2</sub> using equation (1) but uses the observed ozone concentration, measured temperature to evaluate the reaction rates, photochemical equilibrium expressions to calculate [ClO] and [HO<sub>2</sub>], and a delta-Eddington radiative transfer routine to find  $J_{\text{NO}_2}$ , as well as the photolysis rates of other species. Sensitivity studies with this model indicate that  $J_{\text{NO}_2}$  is not sufficiently sensitive to ground albedo or ozone column to significantly diminish the discrepancy between observed and modeled NO/NO<sub>2</sub> shown in Figure 13. Although the radiative routines of the simple and three-dimensional model both included multiple scattering from molecules, neither included scattering from aerosols. This effect is likely to be small at the solar zenith angles characteristic of the latter part of the flight and tends to increase

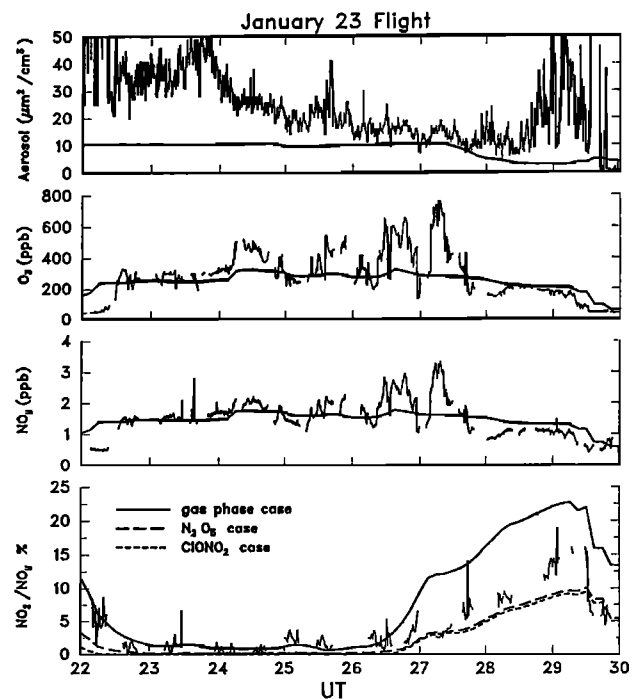


**Figure 7.** Tracers and NO<sub>2</sub>/NO<sub>y</sub> during the January 23 flight.

## Back Trajectories for Jan. 23 Flight

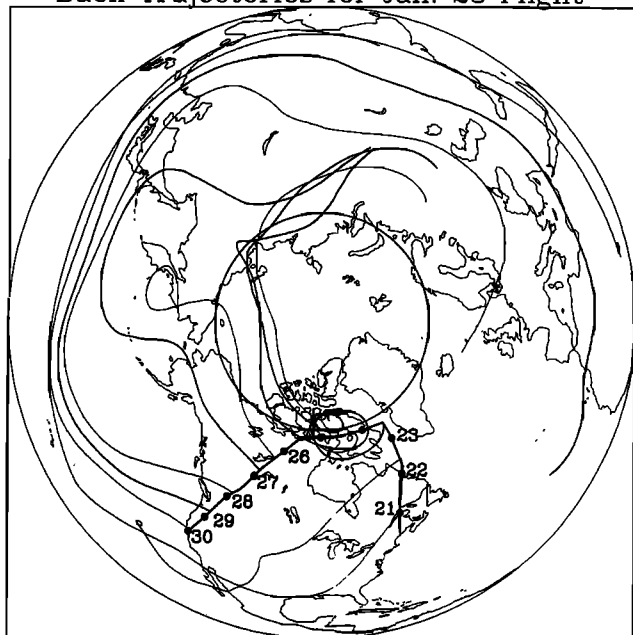


**Figure 8.** Eight-day back trajectories during the January 23 flight.

$J_{\text{NO}_2}$ , so that if included would have made the discrepancy bigger.

## Discussion

For the most part, the NO<sub>x</sub> measurements in the polar night are much less useful than those in midlatitudes for discriminating between the gas phase and the aerosol model runs. This is because both runs predict extremely small NO<sub>x</sub>/NO<sub>y</sub> ratios in the polar night. The fact that the measurements in this region often approach the resolution of the instrument also renders their interpretation more difficult. During the January 16 flight over the north pole, observed NO<sub>x</sub>/NO<sub>y</sub> was larger than all three model simulations. Possible explanations include the following: there is some process regenerating NO<sub>2</sub> in the polar night; the accepted value of the  $k_3$  reaction rate needs revision; or NO<sub>2</sub> is being created within the instrument. At present there is insufficient evidence to distinguish between these or other alternatives. There does not appear to be any single explanation capable of reproducing all of the observed NO<sub>x</sub>/NO<sub>y</sub> variability in the polar night. Analysis of back trajectories is helpful because it indicates that some of the unexplained variability is correlated with past exposure to sunlight.

With the exception of the ambiguous January 14 flight, all the midlatitude comparisons favor the existence of the N<sub>2</sub>O<sub>5</sub> aerosol reaction. This was particularly true of the March comparisons when the simulation using only gas phase chemistry predicted NO<sub>x</sub>/NO<sub>y</sub> ratios so large as to be completely outside the range of observations. The agreement was imperfect how-

ever because this simulation tended to underpredict NO<sub>x</sub>/NO<sub>y</sub>. Whenever the DC-8 flew in sufficient sunlight so that model comparisons with both NO/NO<sub>y</sub> and NO<sub>2</sub>/NO<sub>y</sub> could be made, the N<sub>2</sub>O<sub>5</sub> run simulated NO/NO<sub>y</sub> extremely well but had less NO<sub>2</sub> than observed. The inconsistency between modeled and measured NO<sub>x</sub>/NO<sub>y</sub> therefore arose from a model underestimate of NO<sub>2</sub>/NO<sub>y</sub>. This is disturbing from a theoretical point of view because it seems to imply that the model lacked two distinct physical processes: a mechanism for converting NO<sub>2</sub> to NO and a mechanism for creating NO<sub>x</sub>. In the rest of this section we assume that the N<sub>2</sub>O<sub>5</sub> reaction is in effect and discuss some of the possible reasons for these discrepancies.

Many of the observed NO<sub>2</sub>/NO<sub>y</sub> ratios compare extremely favorably to the (HO<sub>2</sub>NO<sub>2</sub> + NO<sub>2</sub>)/NO<sub>y</sub> ratios of the simulation with the N<sub>2</sub>O<sub>5</sub> aerosol reaction. Of the six flights discussed here, this was true of the flights on January 14 and 23 and March 12 and 20. For these flights the hypothesis that HO<sub>2</sub>NO<sub>2</sub> was being measured by the NO<sub>2</sub> detector with the same efficiency as NO<sub>2</sub> itself was able to resolve both the model overestimate of NO/NO<sub>2</sub> and the underestimate of NO<sub>x</sub>/NO<sub>y</sub>, while retaining the good agreement observed NO/NO<sub>y</sub>. The production of NO<sub>2</sub> within the instrument from thermal decomposition, or photolysis, of HO<sub>2</sub>NO<sub>2</sub> is likely to be negligible given HO<sub>2</sub>NO<sub>2</sub> levels in the range of those calculated by the model. It appears that the only possibility whereby this may occur is via a process occurring on the walls of the inlet tube or glass photolysis cell. Recent laboratory experiments have shown that HO<sub>2</sub>NO<sub>2</sub> can decompose to HONO and HNO<sub>3</sub> on surfaces [Zhu *et al.*, 1993]. HONO photolyzes more readily

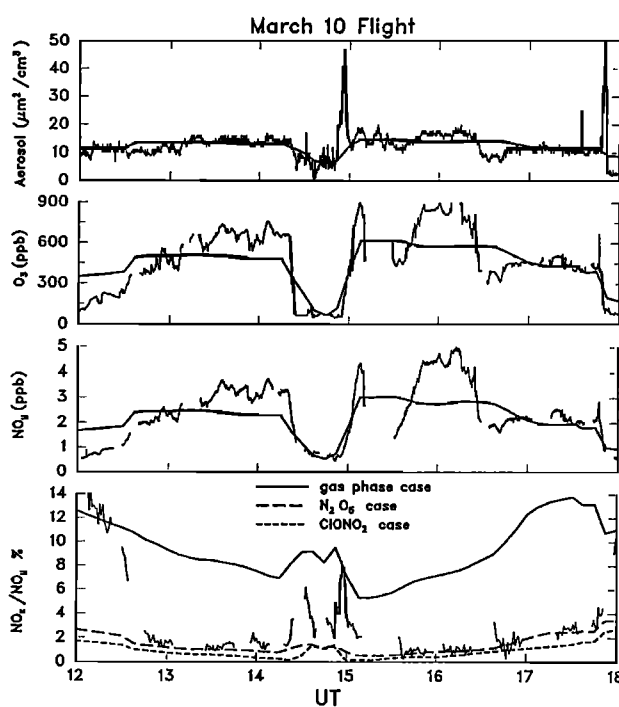


**Figure 9.** Tracers and NO<sub>2</sub>/NO<sub>y</sub> during the March 10 flight.

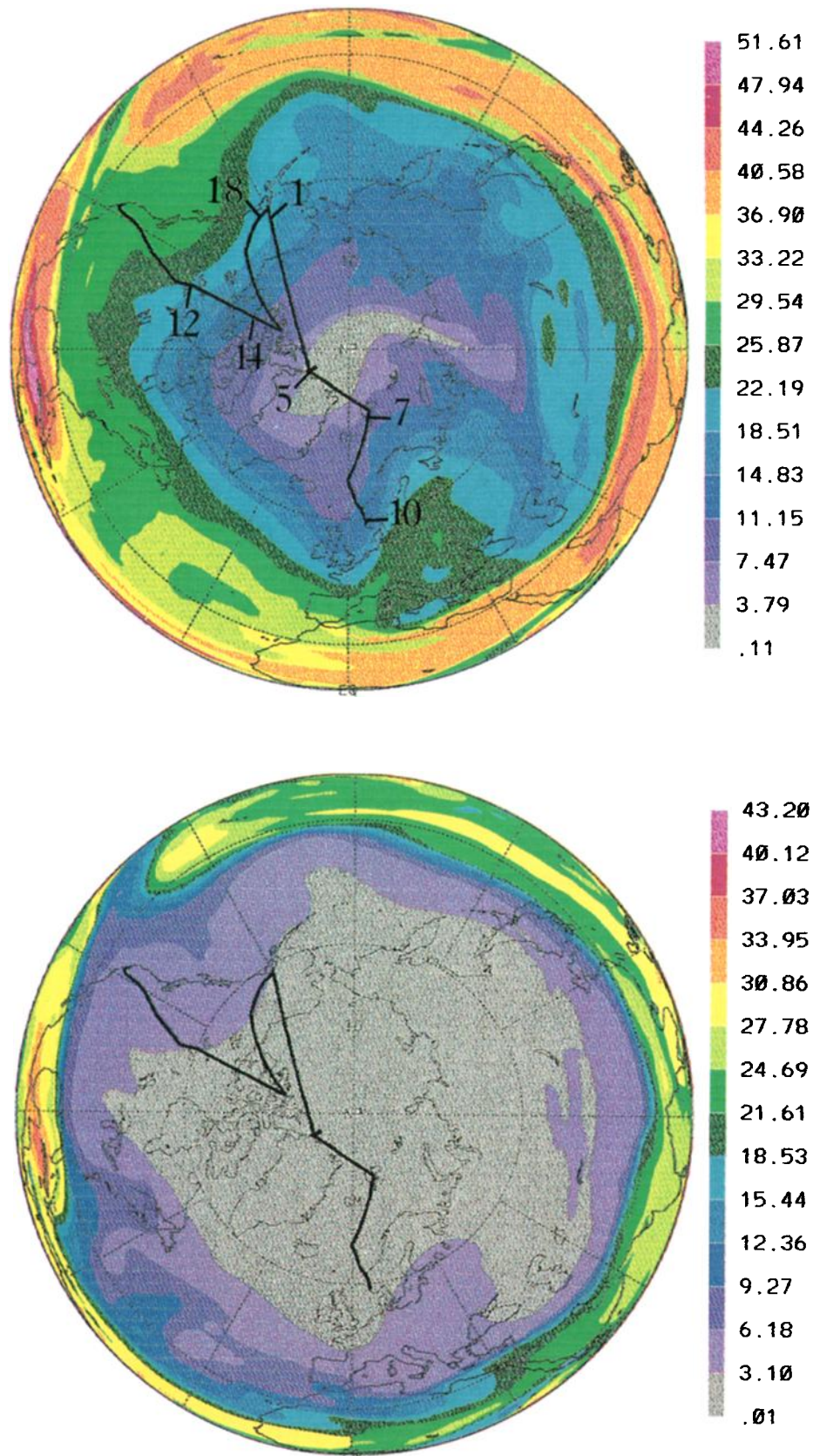


**Plate 2.** Model NO<sub>x</sub>/NO<sub>y</sub> on the 12 km surface at 0000 UT March 11 for the (a) gas phase run and (b) N<sub>2</sub>O<sub>5</sub> aerosol run. The paths of the March 10 flight from Moffett Field to Anchorage and the March 12 flight from Anchorage to Stavanger are shown.

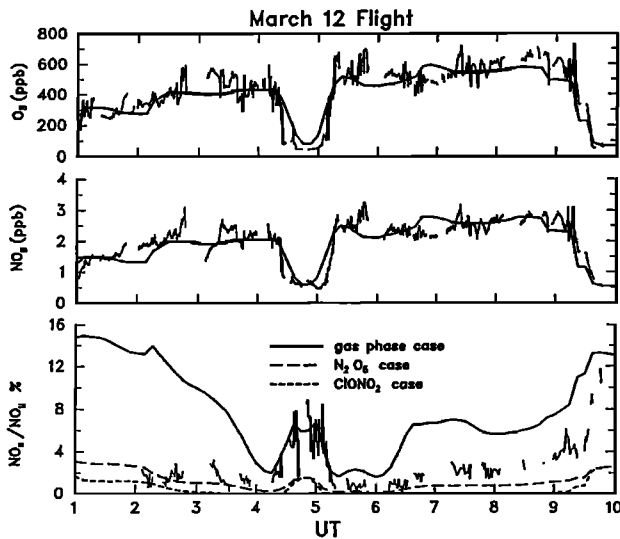


**Figure 10.** Tracers and NO<sub>2</sub>/NO<sub>y</sub> during the March 12 flight. Aerosol surface area during this flight is not available.

than HO<sub>2</sub>NO<sub>2</sub> but approximately 6 times more slowly than NO<sub>2</sub> within the glass photolysis cell, so that this reaction by itself is unable to resolve all of the discrepancies.

It is conceivable that aircraft exhaust effluents are enhancing NO<sub>x</sub>/NO<sub>y</sub> ratios in the lower stratosphere. Modeling results suggest that this is the case in the upper troposphere [Ehhalt *et al.*, 1992; Kasibhatla, 1993], and some of the spikes in the NO<sub>x</sub> data are probably attributable to this source. Any conclusions regarding the effect of this continual injection of NO<sub>x</sub> on NO<sub>x</sub>/NO<sub>y</sub> ratios in the lower stratosphere will be strongly affected by the existence of the N<sub>2</sub>O<sub>5</sub> aerosol reaction. If this reaction is present, then new equilibrium NO<sub>x</sub>/NO<sub>y</sub> ratios are established fairly quickly in air masses exposed to these effluents. This is particularly true in the saturated regime characteristic of the time period in which the DC-8 measurements were made. In this case, one would consider aircraft exhaust to be a source of NO<sub>y</sub>, but a source of NO<sub>x</sub> only in the sense that it enhanced NO<sub>y</sub>. The comparisons between modeled and measured NO<sub>x</sub>/NO<sub>y</sub> given here would then be largely unaffected by the presence of airplane exhaust since the model NO<sub>y</sub> initialization was based on observed NO<sub>y</sub>. If, on the other hand, only gas phase reactions are present, the timescale for NO<sub>x</sub>/NO<sub>y</sub> equilibrium to be reached after an injection of NO<sub>x</sub> is much longer. The emitted NO<sub>x</sub> might be converted to N<sub>2</sub>O<sub>5</sub> relatively quickly, as in the aerosol case, but this N<sub>2</sub>O<sub>5</sub> will then interconvert with NO<sub>x</sub> on a daily timescale for several weeks, rather than being immediately converted to HNO<sub>3</sub>. The magnitude of the aircraft exhaust NO<sub>x</sub> source is in this case more likely to be sufficiently large to enhance NO<sub>x</sub>/NO<sub>y</sub> ratios on a hemispheric scale. However, because our model results largely support the existence of the N<sub>2</sub>O<sub>5</sub> aerosol reaction at DC-8 flight altitudes, this is unlikely to be the case.

To our knowledge, polar stratospheric clouds (PSCs) have never been demonstrated to exist at DC-8 altitudes. It is possible however for reactions on ice surfaces to have affected some of the NO<sub>x</sub> measurements, either via the descent of PSC-processed air from higher altitudes or small localized PSC events at DC-8 altitudes. It is difficult to rule out the first possibility because the degree to which air at 10–12 km has been recently mixed with air from higher altitudes has not yet been well quantified. The second possibility is also difficult to discount because PSC occurrence just above the tropopause during the Arctic winter will be very sensitive to water vapor mixing ratios, which possess a large vertical gradient in this region and which were not measured from the DC-8. However, the seasonal variation of the measured DC-8 NO<sub>x</sub>/NO<sub>y</sub> ratios is inconsistent with the hypothesis that it is PSC rather than aerosol reactions that are giving rise to the large-scale decrease of this ratio from that predicted by gas phase reactions. The comparisons which most strongly support the N<sub>2</sub>O<sub>5</sub> aerosol reaction, those in March, are the comparisons least likely to have been affected by psc reactions.

It is difficult to draw definitive conclusions on the status of the ClONO<sub>2</sub> reaction from our study. This is due to the difficulties of determining NO<sub>x</sub>/NO<sub>y</sub> ratios at extremely low NO<sub>2</sub> concentrations, the fact that ClO concentrations were unknown, and the uncertainty surrounding the model Cl<sub>y</sub> partitioning. The ClONO<sub>2</sub> lifetime against conversion to HOCl at 12 km was of the order of several days. In the model runs where this reaction was included, it led to the creation of a high-ClO and low-NO<sub>x</sub> region centered on the polar night. With

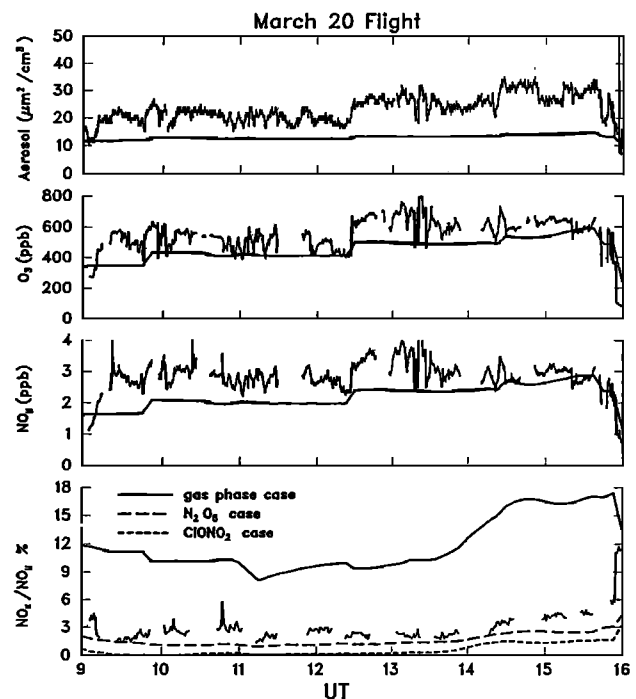


**Figure 11.** Tracers and NO<sub>x</sub>/NO<sub>y</sub> during the March 20 flight.

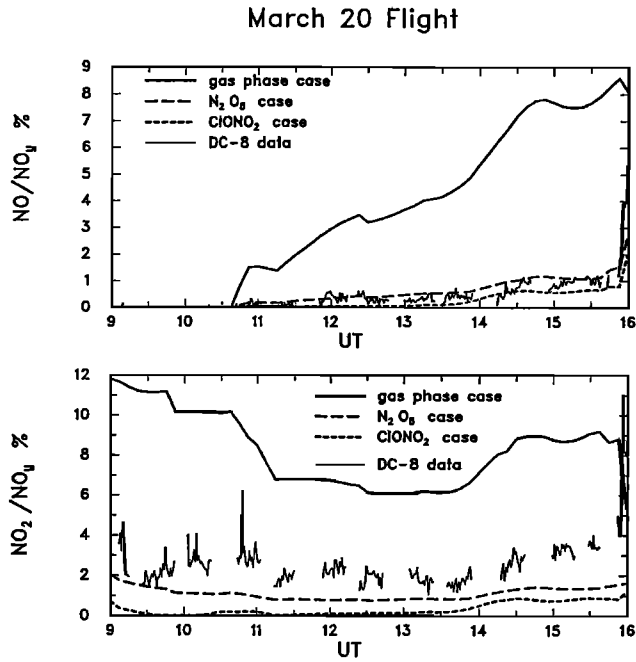


Figure 12.  $\text{NO}/\text{NO}_y$  and  $\text{NO}_2/\text{NO}_y$  during the March 20 flight.

the exception of the fact that HCl was left unchanged, the effect of the  $\text{ClONO}_2$  reaction at these heights was analogous to the effects of reactions on polar stratospheric clouds at higher altitudes. Despite the fact that the DC-8 flew through some of the regions where this had occurred in the  $\text{ClONO}_2$  model run, such low levels of  $\text{NO}_2$  were never observed. This constitutes indirect evidence that the  $\text{ClONO}_2$  reaction was not in effect at

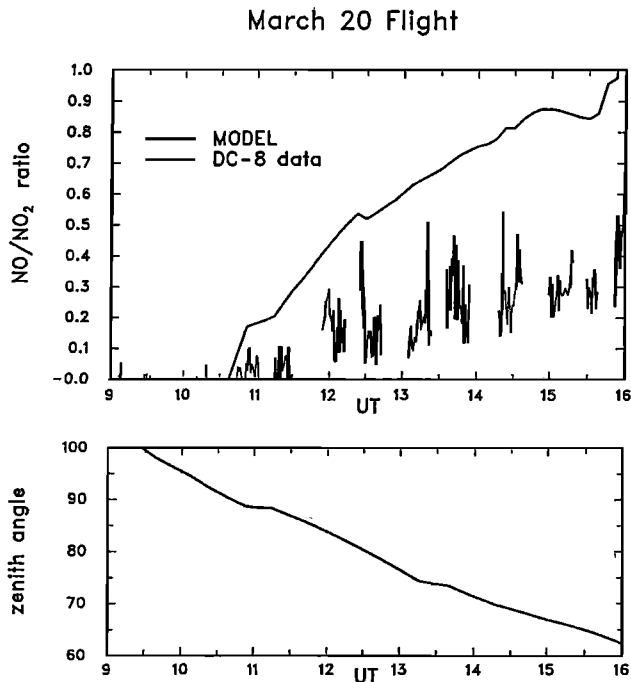


Figure 13. Gas phase model and measured  $\text{NO}/\text{NO}_2$  and solar zenith angle during the March 20 flight.

DC-8 flight levels to the extent suggested by the parameterization of it used here.

$\text{NO}$  was also measured from the ER-2 during AASE 2. These measurements have been used to infer  $\text{NO}_2$  concentrations using an expression similar to equation (1), giving an "observed"  $\text{NO}_x/\text{NO}_y$  ratio. These have been compared to ratios calculated by assuming local steady state [Fahey *et al.*, 1993]. Another approach solved the chemical rate equations along the 10-day back trajectories [Kawa *et al.*, 1993]. Both studies confirmed that the  $\text{N}_2\text{O}_5$  aerosol reaction lowers  $\text{NO}_x/\text{NO}_y$ . The Kawa *et al.* paper showed that taking air parcel histories into account can significantly improve agreement with observed  $\text{NO}_x/\text{NO}_y$ . This is consistent with the figures given here showing the zonal asymmetry of modeled  $\text{NO}_x/\text{NO}_y$  and the correlation of these asymmetries with geopotential height. These papers could not make any comparisons between observed and modeled polar night  $\text{NO}_x$  because they were restricted to regions where  $\text{NO}$  concentrations were measurable. Many of the discrepancies discussed here between observed and modeled  $\text{NO}_x/\text{NO}_y$  and  $\text{NO}/\text{NO}_2$  would not have been identified if inferred, rather than directly measured,  $\text{NO}_2$  had been used.

## Conclusion

The advantage of using a three-dimensional model to interpret aircraft measurements is that it explicitly takes the photochemical histories of the air parcels intersecting the airplane into account and allows stringent comparisons between theory and observations. Comparisons of the DC-8 measurements with this model strongly support the idea that the reaction of  $\text{N}_2\text{O}_5$  with water on aerosol surfaces suppresses  $\text{NO}_x$  levels in the midlatitude lower stratosphere. They also indicate that our understanding of reactive nitrogen chemistry in this region is incomplete. The model tends to consistently underestimate measured  $\text{NO}_x/\text{NO}_y$ . Observed  $\text{NO}/\text{NO}_2$  in this region differs strongly from calculations based on the presently accepted factors controlling this ratio. It is not yet clear whether these discrepancies arise from conversion of other nitrogen species to  $\text{NO}_2$  within the instrument, or the absence from the model of important reactions regulating  $\text{NO}_2$  in the lower stratosphere.

**Acknowledgments.** The National Center for Atmospheric Research (NCAR) is sponsored by the National Science Foundation. The measurements were supported by the NASA High Speed Research Program and (for NCAR) the Upper Atmosphere Research Program. The ECMWF archive at NCAR is maintained by the Data Support Section. We thank Leslie Lait and Randy Kawa for the back trajectory calculations, all those whose measurements were used to initialize the model, including G. Sachse for the CO data, and Peter Hess and Claire Granier for careful readings of the manuscript. I. F. was supported in part by a fellowship from the Natural Sciences and Engineering Research Council of Canada.

## References

- DeMore, W. B., S. P. Sander, C. J. Howard, A. R. Ravishankara, D. M. Golden, C. E. Kolb, R. F. Hampson, M. J. Kurylo, and M. J. Molina, Chemical kinetics and photochemical data for use in stratospheric modeling, In evaluation 10, *JPL Pub. 92-20*, Jet Propulsion Lab., Pasadena, Calif., 1992.
- Douglass, A. R., R. B. Rood, R. S. Stolarski, M. R. Schoeberl, M. H. Proffitt, J. J. Margitan, M. Loewenstein, J. R. Podolske, and S. E. Strahan, Global three-dimensional constituent fields derived from profile data, *Geophys. Res. Lett.*, **17**, 525-528, 1990.
- Ehhalt, D. H., F. Rohrer, and A. Wahner, Sources and distribution of NO<sub>x</sub> in the upper troposphere at northern midlatitudes, *J. Geophys. Res.*, **97**, 3725-3738, 1992.
- Fahey, D. W., et al., In situ measurements constraining the role of reactive nitrogen and sulphate aerosols in mid-latitude ozone depletion, *Nature*, **363**, 509-514, 1993.
- Gaines, S., P. Hataway, and S. Hipskind, (Eds.), Airborne Arctic Stratospheric Expedition II, *CD-ROM NASA/UARP-004*, NASA Ames Research Center, Moffett Field, Calif., 1992.
- Granier, C., and G. Brasseur, Impact of heterogeneous chemistry on model predictions of ozone changes, *J. Geophys. Res.*, **97**, 18015-18033, 1992.
- Hofmann, D. J., and S. J. Oltmans, The effect of stratospheric water vapor on the heterogeneous reaction rate of ClONO<sub>2</sub> and H<sub>2</sub>O for sulfuric acid aerosol, *Geophys. Res. Lett.*, **19**, 2211-2214, 1992.
- Kasibhatla, P. S., NO<sub>y</sub> from sub-sonic aircraft emissions: A global three-dimensional model study, *Geophys. Res. Lett.*, **16**, 1707-1710, 1993.
- Kawa, S. R., et al., Interpretation of NO<sub>x</sub>/NO<sub>y</sub> observations from AASE-II using a model of chemistry along trajectories, *Geophys. Res. Lett.*, **20**, 2507-2510, 1992.
- Kley, D., and M. McFarland, Chemiluminescence detector for NO and NO<sub>2</sub>, *Atmos. Technol.*, **12**, 63-69, 1980.
- Lefèvre, F., G. Brasseur, I. Folkins, A. K. Smith, and Paul Simon, Chemistry of the 1991-1992 stratospheric winter: Three-dimensional model simulations, *J. Geophys. Res.*, **99**, 8183-8191, 1994.
- Prather, M. J., and E. E. Remsberg (Eds.), The atmospheric effects of stratospheric aircraft: Report of the 1992 Models and Measurements Workshop, *NASA Ref. Pub. 1292*, III, 1993.
- Pueschel, R. F., S. A. Kinne, P. B. Russell, and ff. G. Snetsinger, Effects of the Pinatubo volcanic eruption on the physical and radiative properties of stratospheric aerosols, in *Proceedings of the IRS'92 Current Problems in Atmospheric Radiation*, edited by S. Keavallik, pp. 183-186, A. Deepak, Hampton, Va., 1992.
- Ridley, B. A., M. McFarland, A. L. Schmeltekopf, M. H. Proffitt, D. L. Albritton, R. H. Winkler, and T. L. Thompson, Seasonal differences in the vertical distributions of NO, NO<sub>2</sub>, and O<sub>3</sub> in the stratosphere near 50°N, *J. Geophys. Res.*, **92**, 11,919-11,929, 1987.
- Rodriguez, J. M., M. K. W. Ko, and N. D. Sze, Role of heterogeneous conversion of N<sub>2</sub>O<sub>5</sub> on sulphate aerosols in global ozone losses, *Nature*, **352**, 134-137, 1991.
- Schoeberl, M. R., et al., Reconstruction of the constituent distribution and trends in the Antarctic polar vortex from the ER-2 flight observations, *J. Geophys. Res.*, **94**, 16,815-16,845, 1989.
- Solomon, S., J. M. Russell, L. L. Gordley, Observations of the diurnal variation of nitrogen dioxide in the stratosphere, *J. Geophys. Res.*, **91**, 5455-5464, 1986.
- Solomon, S., R. W. Sanders, R. R. Garcia, and J. G. Keys, Increased chlorine dioxide over Antarctica caused by volcanic aerosols from Mount Pinatubo, *Nature*, **363**, 245-248, 1993.
- Walega, J. G., J. E. Dye, F. E. Grahek, and B. A. Ridley, A compact measurement system for the simultaneous determination of NO, NO<sub>2</sub>, NO<sub>y</sub> and O<sub>3</sub> using a small aircraft, in *Measurement of Atmospheric Gases, SPIE Proc., Int. Soc. Opt. Eng.*, 232-240, 1991.
- Webster, C. R., R. D. May, D. W. Toohey, L. M. Avallone, J. G. Anderson, P. Newman, L. Lait, M. R. Schoeberl, J. W. Elkins, and K. R. Chan, Chlorine chemistry on polar stratospheric clouds in the Arctic winter, *Science*, **261**, 1130-1134, 1993.
- World Meteorological Organization (WMO), Scientific Assessment of Ozone Depletion: 1991, Global Ozone Research and Monitoring Project, *WMO Rep. 25*, Geneva, 1992.
- Zhu, T., G. Yarwood, J. Chen, and H. Niki, Evidence for the heterogeneous formation of nitrous acid from peroxyxynitric acid in environmental chambers, *Environ. Sci. Technol.*, **27**, 982-983, 1993.

---

Guy Brasseur, Ian Folkins, Brian A. Ridley, James G. Walega, A.J. Weinheimer, National Center for Atmospheric Research, Boulder, CO 80307.

James E. Collins, Science and Technology Corporation, Hampton, VA 23666.

Frank Lefevre, Météo-France, Centre National de Recherches Météorologiques, Toulouse, France.

R. F. Pueschel, NASA Ames Research Center, Moffett Field, CA 94035.

(Received October 13, 1993; revised May 31, 1994; accepted June 17, 1994.)